



## Tensile and creep properties of an oxide dispersion-strengthened ferritic steel

R.L. Klueh<sup>a,\*</sup>, P.J. Maziasz<sup>a</sup>, I.S. Kim<sup>b</sup>, L. Heatherly<sup>a</sup>, D.T. Hoelzer<sup>a</sup>,  
N. Hashimoto<sup>a</sup>, E.A. Kenik<sup>a</sup>, K. Miyahara<sup>b</sup>

<sup>a</sup> *Metals and Ceramics Division, Oak Ridge National Laboratory, P.O. Box 2008, MS 6151, Oak Ridge, TN 37831, USA*

<sup>b</sup> *Department of Molecular Design and Engineering, Nagoya University, Nagoya, Japan*

### Abstract

The tensile and creep properties of two oxide dispersion-strengthened (ODS) steels with nominal compositions of Fe–12Cr–0.25Y<sub>2</sub>O<sub>3</sub> (designated 12Y1) and Fe–12Cr–2.5W–0.4Ti–0.25Y<sub>2</sub>O<sub>3</sub> (12YWT) were investigated. Optical microscopy, transmission electron microscopy, and atom probe field ion microscopy studies indicated that the 12Y1 contained a high density of extremely fine Y–Ti–O clusters, compared to the much larger oxide particles in the 12Y1. The fine dispersion of particles gave the 12YWT better tensile and creep properties compared to commercial ODS alloys and ferritic/martensitic steels that would be replaced by the new ODS steel.

© 2002 Elsevier Science B.V. All rights reserved.

### 1. Introduction

If the conventional high-chromium ferritic/martensitic steels, such as modified 9Cr–1Mo and Sandvik HT9, or the reduced-activation steels, such as F82H, ORNL 9Cr–2WVTa, and JLF-1, were used for a fusion power plant first wall and blanket structure, the upper operating temperature would be limited to 550–600 °C. One way suggested to increase this limit to 650 °C or higher and maintain the advantages inherent in ferritic/martensitic steels (i.e. high thermal conductivity and low swelling) is to use oxide dispersion-strengthened (ODS) steels. Elevated temperature strength in these steels is obtained through microstructures that contain a high density of small Y<sub>2</sub>O<sub>3</sub> or TiO<sub>2</sub> particles dispersed in a ferrite matrix.

ODS steels are being developed and investigated for fission and fusion applications in Japan [1,2], Europe [3,4], and the United States [5–7]. This paper will summarize some preliminary mechanical properties work

conducted on two ODS steels produced by Kobe Steel Ltd.

### 2. Experimental

Nominal compositions (in wt%) of the ODS steels examined were Fe–12Cr–0.25Y<sub>2</sub>O<sub>3</sub> (designated 12Y1) and Fe–12Cr–2.5W–0.35Ti–0.25Y<sub>2</sub>O<sub>3</sub> (12YWT). The actual composition of 12Y1 was Fe–12.9Cr–0.25Ni–0.04Mn–0.03Mo–0.03Si–0.045C–0.2Y–0.15O, and the composition of the 12YWT was Fe–12.6Cr–2.44W–0.27Ni–0.1Si–0.05Mn–0.02Mo–0.052C–0.35Ti–0.16Y–0.16O. Both alloys were prepared by mechanically alloying 70 μm diameter, argon-atomized, pre-alloyed metal powders and 20 nm Y<sub>2</sub>O<sub>3</sub> powder. The process involved milling in a high-energy attritor mill in an argon atmosphere. After the mechanical alloying step, the flakes were degassed and consolidated into a bar by hot extrusion at 1150 °C. Further processing by hot and cold rolling interspersed with annealing treatments was used to convert the extruded bar into sheet with a final thickness of 2 mm [7].

Sheet tensile specimens 1.5 mm thick and 38 mm long with a 12.7 mm × 3.1 mm × 1.5 mm gage section were

\* Corresponding author. Tel.: +1-865 574 5111; fax: +1-865 574 0641.

E-mail address: [kluehrl@ornl.gov](mailto:kluehrl@ornl.gov) (R.L. Klueh).

machined in the longitudinal orientation for uniaxial tensile and creep tests. Tensile tests were conducted in air over the range room temperature to 900 °C at  $3.3 \times 10^{-3} \text{ s}^{-1}$ . Creep tests in air were made over the range 600–850 °C.

Microstructures were examined by optical microscopy, transmission electron microscopy (TEM), and scanning electron microscopy (SEM) using conventional techniques.

### 3. Results and discussion

#### 3.1. Microstructure

Optical microstructures of the 12Y1 and 12YWT showed some significant differences. The 12YWT had a much smaller grain size compared to the 12Y1. Both steels exhibited elongated grains that were generally consistent with unidirectional rolling and grain growth and coalescence during annealing. The grain size and aspect ratio of the 12Y1 were estimated at 2–5  $\mu\text{m}$  and 3–5, respectively, and for the 12YWT they were estimated at 0.4–2  $\mu\text{m}$  and 10–15, respectively. No transverse measurements of mechanical properties have been performed to determine the effect of the elongated grains.

TEM microstructures of as-processed 12Y1 and 12YWT were considerably different (Fig. 1). The 12YWT contained up to an order of magnitude more dislocations pinned by a fairly uniform distribution of very fine particles, whereas the 12Y1 contained much larger particles less uniformly distributed. For the 12Y1, particles

were estimated to be 10–40 nm in diameter at a number density of  $10^{20}$ – $10^{21} \text{ m}^{-3}$ ; the dislocation density was estimated at  $\approx 10^{15} \text{ m}^{-2}$  [6]. Diffraction studies indicated that the particles in the 12Y1 were crystalline, and XEDS analysis of the particles on carbon film extraction replicas indicated they were essentially pure  $\text{Y}_2\text{O}_3$ . For the 12YWT, the dislocation density, particle size, and particle number density were estimated at  $10^{15}$ – $10^{16} \text{ m}^{-2}$ , 3–5 nm diameter, and  $1\text{--}2 \times 10^{23} \text{ m}^{-3}$ , respectively. It was not possible to identify these particles by electron diffraction because they were too small; no spots or amorphous rings were observed [6]. Carbon film extraction replicas from the 12YWT failed to extract these fine particles (presumably because they dissolved), while XEDS of coarse particles showed Cr-, Ti-, Fe-rich oxides with no trace of  $\text{Y}_2\text{O}_3$ .

To determine the nature of the extremely fine particles in the 12YWT, atom probe field ion microscopy studies were conducted. The three-dimensional atom probe (3-DAP) analysis of random volumes revealed compositionally distinct nano-sized clusters in the 12YWT that were not present in the 12Y1 [7]. The matrix of the 12Y1 contained low levels of Y and O but no indication of clustering. In contrast to this, the 12YWT contained many clusters enriched in Y, Ti, and O, slightly enriched in Cr, and slightly depleted in Fe and W. More recent quantitative analysis of 3-DAP results indicated an average diameter of 2.6 nm, a size range of 1–5 nm and a cluster concentration of  $1.1 \times 10^{24} \text{ m}^{-3}$  [8].

From the atom probe data and analysis, it was concluded that the original  $\text{Y}_2\text{O}_3$  particles had evidently dissolved during the processing of the alloy, and that

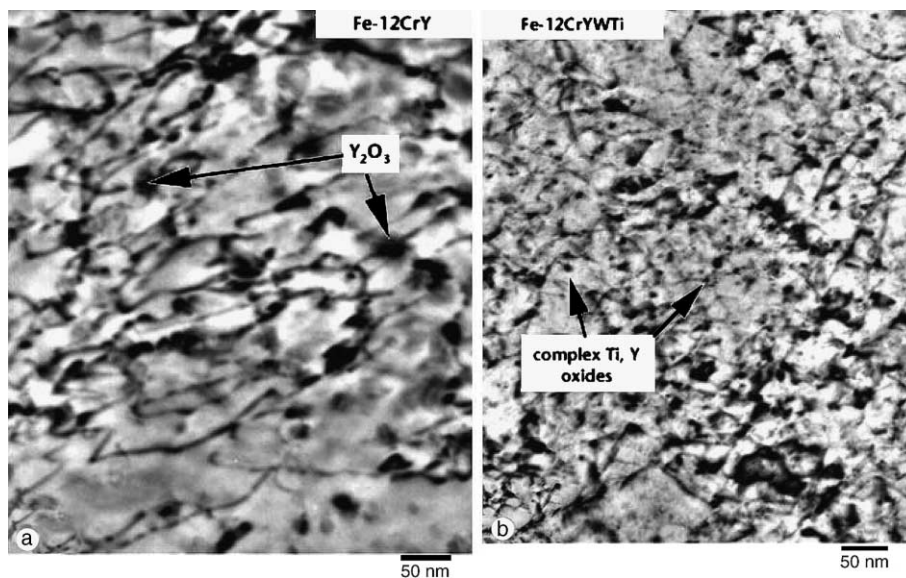


Fig. 1. Transmission electron micrographs of (a) Fe–12Cr–0.25Y<sub>2</sub>O<sub>3</sub> (12Y1) and (b) Fe–12Cr–2.5W–0.4Ti–0.25Y<sub>2</sub>O<sub>3</sub> (12YWT) steels.

new, small clusters then formed. The appearance of the titanium in the clusters indicated that it must play a critical role in the dissolution process. At what point in the processing of the ODS steel the dissolution and subsequent clustering occurred still needs to be established.

### 3.2. Tensile properties

In Fig. 2(a), the 0.2% yield stress from room temperature to 900 °C is shown for 12Y1 and 12YWT. For comparison, data for the reduced-activation 9Cr–2WVTa steel is also shown for tests from room temperature to 700 °C [8]; the strength of this steel decreases rapidly above 600 °C, which is near the limit for such a steel. The superior strength of the 12YWT over the 12Y1 is obvious in this figure, and this is consistent with the difference expected based on the large difference in the microstructures. Indeed, because of the much larger and

less evenly distributed oxide particles in the 12Y1, the yield stress of this steel is only higher than that of the 9Cr–2WVTa steel below  $\approx 550$  °C, while the 12YWT continues to show excellent strength well above this temperature.

The total elongations for 12Y1 and 12YWT are shown in Fig. 2(b) (no elongations are shown for the 9Cr–2WVTa because this steel was tested in another experiment, and different specimen geometries were used [9]). As expected from the relative yield stress behavior, the elongation of the weaker 12Y1 exceeded that of the 12YWT. However, despite the higher strength, the 12YWT still had good ductility.

### 3.3. Creep properties

The most important property for any structural material expected to operate at elevated temperatures is thermal creep. Creep tests were conducted on the 12Y1 and 12YWT at 600–850 °C, and the 12YWT has excellent creep resistance over this temperature range. Fig. 3 presents a Larson–Miller diagram that compares the 12YWT with 12Y1 and other ODS [5] and conventional steels. In this figure, the stress to rupture is plotted against the Larson–Miller parameter (LMP), which is defined as  $LMP = T(25 + \log t)$ , where  $T$  is the temperature in Kelvin and  $t$  is the rupture time in hours.

It is obvious from Fig. 3 that the creep-rupture behavior of the 12YWT is superior to the other materials, which are: 12Y1, MA956 (Fe–19Cr–0.33Ti–5Al–0.4Y–0.15O–0.02C) and MA957 (Fe–14Cr–0.3Mo–1Ti–0.3Y–0.2O–0.03C), the latter two being commercial ODS steels, and 9Cr–WMoVNb, which is a commercial

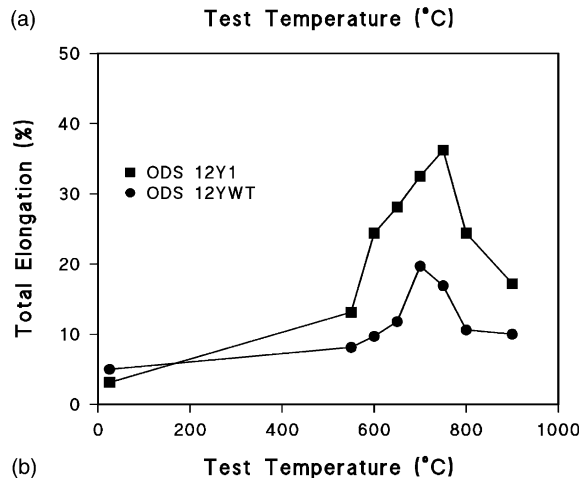
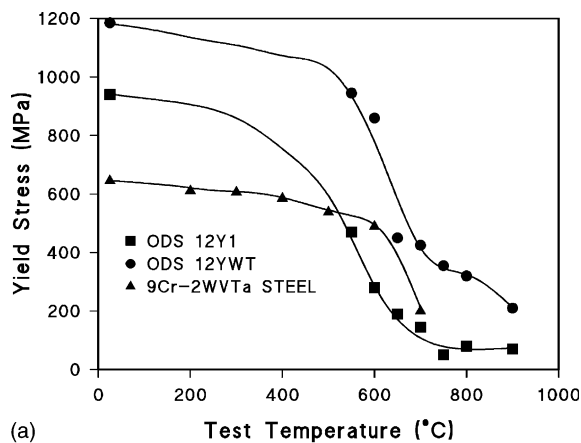


Fig. 2. (a) The 0.2% yield stress of the 12Y1 and 12YWT ODS steels and the reduced-activation 9Cr–2WVTa steel and (b) the total elongation of the 12Y1 and 12YWT.

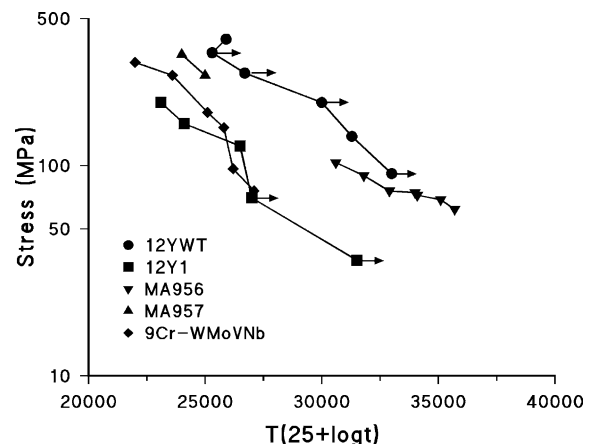


Fig. 3. Larson–Miller diagram for the creep-rupture strength of four ODS steels and a conventional ferritic/martensitic steel. The arrows indicate that the test is still in progress, or it was discontinued prior to rupture.

ferritic/martensitic steel. Since only a few of the tests for 12YWT in Fig. 3 have ruptured, the curve for the 12YWT should eventually exceed that of all the other materials for all test conditions.

In Fig. 4, a typical creep curve is shown for the 12YWT tested at 800 °C at 138 MPa, and it is compared with a curve for the V-4Cr-4Ti alloy [10], another candidate for fusion applications at temperatures above 600 °C. The V-4Cr-4Ti was also tested at 800 °C but at a much lower stress – 77 MPa (the V-4Cr-4Ti alloy test is from a biaxial creep test using a pressurized tube). Whereas the vanadium alloy creep curve is in the tertiary creep stage prior to rupture (the specimen failed after 4029 h and  $\approx 52\%$ ), the 12YWT steel at  $\approx 5000$  h appears to be in the steady-state creep stage (Fig. 4). This specimen ruptured after  $\approx 14\,500$  h (800 °C is an extremely high temperature for a steel with only 12% Cr) with an elongation  $\approx 2.3\%$ , but it failed without a tertiary creep stage.

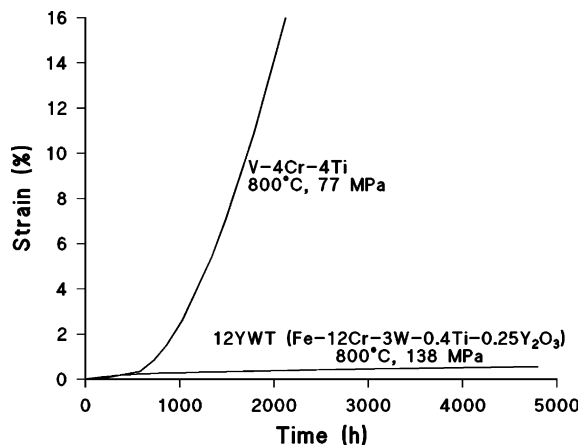


Fig. 4. A comparison of the creep behavior of the ODS steel 12YWT and the V-4Cr-4Ti alloy.

The microstructure of the 12YWT creep specimen that failed after 14 500 h at 800 °C was examined by TEM and SEM. The TEM showed a high density of dislocations along with clear depiction of the elongated grain structure of the material developed by the processing procedure (Fig. 5). Observations by SEM on polished specimens further elucidated the grain structure (Fig. 6). In particular, the as-processed specimen again showed the elongated grain structure (Fig. 6(a)). The crept specimen (Fig. 6(b)) also gave an indication of the elongated grain structure (note that this SEM specimen was a thinned TEM specimen, and the black region in the center of the figure is the hole), but in addition, indications of recrystallization were observed. Such evidence of recrystallization was still only apparent in isolated regions, suggesting that recrystallization was in its initial stages for this specimen creep tested at 800 °C for  $\approx 14\,500$  h. No unstressed specimens have been



Fig. 5. Transmission electron micrograph of 12YWT after creep for  $\approx 14\,500$  h at 800 °C and 138 MPa.

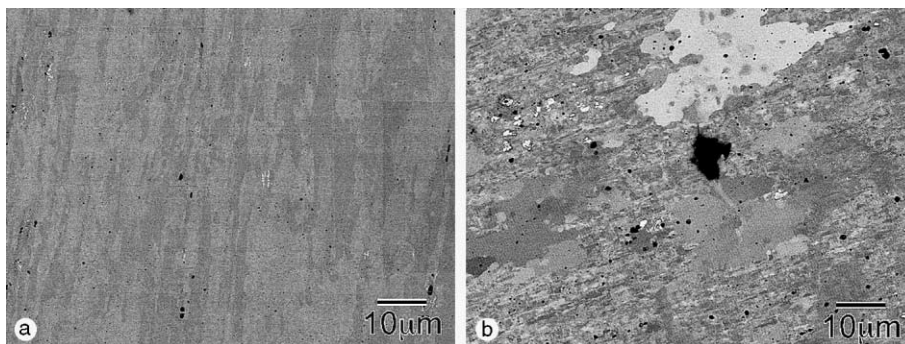


Fig. 6. Scanning electron micrograph of 12YWT (a) as processed and (b) after creep for  $\approx 14\,500$  h at 800 °C.

thermally aged to determine the role of stress in the recrystallization.

#### 4. Conclusion

Preliminary microstructural studies of an Fe–12Cr–2.5W–0.4Ti–0.25Y<sub>2</sub>O<sub>3</sub> ODS steel demonstrated that this steel has a distribution of extremely fine (nano-sized) clusters that are very stable and give the steel excellent elevated-temperature tensile and creep properties relative to other ODS steels and conventional and reduced-activation ferritic/martensitic steels. The preliminary creep properties of 12YWT also appear to be superior to those of the V–4Cr–4Ti alloy, although the creep-rupture elongation was quite low.

It must be emphasized that even though the 12YWT steel displays these excellent properties, ODS steels for fusion are still at an early development stage, similar to the vanadium alloys. Neither of these materials is at a commercial stage of development comparable to conventional and reduced-activation ferritic/martensitic steels, for which the technology (i.e. steel processing, final fabrication, welding, etc.) is advanced to the point that a fusion reactor could be constructed. Some of the problems still to be solved for ODS steels include: the elimination of the elongated grain structure (deriving from the way the steels are processed) that produces anisotropic behavior in the mechanical properties, the production of large section sizes, and the joining of ODS steels in a large structure. Finally, there is the question of irradiation resistance of ODS steels, for which limited information is available.

#### Acknowledgements

Research sponsored by the Office of Fusion Energy Sciences, Laboratory Directed Research and Development Program, and the Division of Materials Sciences and Engineering, US Department of Energy, under contract DE-AC05-00OR22725 with UT-Battelle, LLC.

#### References

- [1] S. Ukai, T. Nishida, H. Okada, T. Okuda, M. Fujiwara, K. Asabe, *J. Nucl. Sci. Technol.* 34 (1997) 256.
- [2] S. Ukai, T. Yoshitake, S. Mizuta, Y. Matsudaira, S. Hagi, T. Kobayashi, *J. Nucl. Sci. Technol.* 36 (1999) 710.
- [3] A. Alamo, J. Decours, M. Pigoury, C. Foucher, in: *Structural Applications of Mechanical Alloying*, ASM International, Materials Park, OH, 1990.
- [4] A. Alamo, H. Regle, G. Pons, L.L. Bechade, *Mater. Sci. Forum* 88–90 (1992) 183.
- [5] D.K. Mukhopadhyay, F.H. Froes, D.S. Gelles, *J. Nucl. Mater.* 258–263 (1998) 1209.
- [6] I.-S. Kim, J.D. Hunn, N. Hashimoto, D.L. Larson, P.J. Maziasz, K. Miyahara, E.H. Lee, *J. Nucl. Mater.* 280 (2000) 264.
- [7] D.J. Larson, P.J. Maziasz, I.-S. Kim, K. Miyahara, *Scripta Mater.* 44 (2001) 359.
- [8] E.A. Kenik, D. Hoelzer, P.J. Maziasz, M.K. Miller, in: G.W. Bailey, R.L. Price, E. Voelkl, I.H. Musselman (Eds.), *Microscopy and Microanalysis 2001*, Springer, New York, 2001, p. 550.
- [9] R.L. Klueh, *Met. Trans.* 20A (1989) 463.
- [10] R.J. Kurtz, M.L. Hamilton, *Fusion Materials Semiannual Progress Report for Period Ending 30 June 1999*, DOE/ER-0313/26, September 1999, p. 3.